JOURNAL OF SOLID STATE CHEMISTRY 103, 216–227 (1993)

La_2O_3–CuO–TiO_2 Phase Diagram and the Crystal Structure of $[La_{0.86}\square_{0.14}Cu_3](Ti_{3.42}Al_{0.58})O_{12}$[1]

MARK T. ANDERSON,*,† VINCENT E. BALBARIN,*,†,[2]
DAWN A. GROENKE,*,† GORDON A. BAIN,* AND
KENNETH R. POEPPELMEIER*,†,[3]

Department of Chemistry and the †Science and Technology Center for Superconductivity, Northwestern University, Evanston, Illinois 60208

Received May 19, 1992; in revised form August 31, 1992; accepted September 3, 1992

The La_2O_3–CuO–TiO_2 system in air at 960°C contains two perovskite-related ternary compounds, La_2CuTiO_6 and $\{La_{2/3}\square_{1/3}Cu_3\}(Ti_4)O_{12}$. The former is orthorhombic, has cell parameters a = 5.587 (6), b = 5.616 (5), c = 7.842 (7) Å, is isostructural with $GdFeO_3$, and exhibits Curie–Weiss magnetic behavior. The copper and titanium are statistically distributed over one crystallographic site. The La_2O_3–CuO–TiO_2 and La_2O_3–CuO–SnO_2 systems differ in their phase relationships, number of ternary phases, and crystal chemistry of their La_2CuMO_6 (M = Ti, Sn) compounds. Single crystals of $[La_{0.86}\square_{0.14}Cu_3](Ti_{3.42}Al_{0.58})O_{12}$ were grown in an Al_2O_3 crucible from a CuO–TiO_2 flux and crystallize in the cubic space group $Im\bar{3}$ with a = 7.421 (1) Å and Z = 2. The compound is isostructural with $[CaMn_3](Mn_4)O_{12}$. The excess lanthanum in the crystal compensates the charge deficiency brought about by the aluminum incorporation, and the electrostatic stabilization it affords is the principal driving force for the observed structure. © 1993 Academic Press, Inc.

Introduction

Phase diagram studies of copper–oxygen systems have played an integral role in the discovery and isolation of superconductors. We recently investigated the La_2O_3–CuO–SnO_2 system and discovered the new perovskite-related material La_2CuSnO_6 (*1*). The material is of interest because it is the only stoichiometric perovskite $A_2B'B''O_6$ that contains distinct $B'O_2$ and $B''O_2$ layers. Its unique B-cation arrangement prompted further investigation of A_2O_3–CuO–BO_2 systems. The La_2O_3–CuO–TiO_2 system has been investigated because of the similar coordination chemistry and structural preferences of tin and titanium oxides (*2*, *3*). Our goal is to determine the effect that replacement of tin by titanium has on the phase relationships and phase formation in the La_2O_3–CuO–BO_2 system, as well as the effect it has on the crystal chemistry and physical properties of the compounds in the system. We present results of the phase

[1] See NAPS document No. 04987 for 03 pages of supplementary material. Order from ASIS/NAPS. Microfiche Publications, P.O. Box 3515, Grand Central Station, New York, NY 10163. Remit in advance $4.00 for microfiche copy or for photocopy, $7.75 up to 20 pages plus $.30 for each additional page. All orders must be prepaid. Institutions and Organizations may order by purchase order. However, there is a billing and handling charge for this service of $15. Foreign orders add $4.50 for postage and handling for the first 20 pages, and $1.00 for additional 10 pages of material, $1.50 for postage and any microfiche orders.

[2] Present address: Baker Laboratory, Department of Chemistry, Cornell University, Ithaca, New York 14853.

[3] To whom correspondence should be addressed.

0022-4596/93 $5.00

diagram study, the crystal structure of $[La_{0.86}\square_{0.14}Cu_3](Ti_{3.42}Al_{0.58})O_{12}$, the crystal chemistry of La_2CuTiO_6, and a general discussion of the differences between the tin and titanium systems.

Experimental

Synthesis and Characterization of Polycrystalline Samples

La_2CuTiO_6 and specimens for the phase study were prepared by solid-state reaction of copper(II) oxide (99.99+%), titanium(IV) oxide (99.9+%), and lanthanum oxide (99.99%). The materials were heated in high density alumina boats in air at 960°C for 21 to 56 days. This temperature was sufficient to lessen reaction time yet low enough to prevent melting of the samples (*4*). The progress of the reactions was monitored every 3 to 7 days by the use of X-ray diffraction methods. The samples were quenched in air, ground, and pressed into pellets each time X-ray diffraction was performed.

Susceptibility Measurements

A Quantum Design Corporation MPMS SQUID susceptometer was employed to record magnetic data between 5 and 300 K. The applied magnetic field was 1000 G. The measurements were performed on finely ground samples that were contained in sealed gelatin capsules. The data were corrected for the diamagnetism of the sample holder. A platinum metal standard was used for instrument calibration.

Single Crystal Studies

Crystal growth and chemical analysis. Dark purple cubic crystals of $[La_{(2+x)/3}\square_{(1-x)/3}Cu_3](Ti_{1-x}Al_x)O_{12}$ were grown in an Al_2O_3 crucible from a high-temperature solution of CuO–TiO_2–La_2O_3 (108 : 54 : 10 ratio). The mixture was heated in air to 1100°C, allowed to soak for 8 h, cooled at 6°/h to 700 °C, and quenched to room temperature (~200°C/min). The crucible was broken open; this procedure resulted in many free crystals. A Hitachi S570 scanning electron microscope equipped with a Tracor Northern energy dispersive X-ray spectrometer revealed that the crystals contained lanthanum, copper, titanium and aluminum in the approximate ratio 10 : 37 : 48 : 5. The stoichiometry was established from the refinement.

X-ray diffraction. An Enraf–Nonius CAD-4 diffractometer was used to collect intensity data on a crystal with the approximate dimensions 0.14 × 0.12 × 0.14 mm. The cell constants were determined from least-squares analysis of 25 reflections collected in the range $24.7° < 2\theta < 35.2°$. The systematic absence $h + k + l = 2n + 1$ indicated a cubic body-centered cell. A total of 1071 reflections were collected of which 361 were unique ($R_{int} = 0.063$). Three representative reflections were monitored at 45-min intervals and exhibited no significant variation of intensity throughout the collection. A summary of the experimental details and crystallographic data is presented in Table I.

The data were corrected for Lorentz and polarization effects, and an analytical absorption correction (*5*) based on the indexed faces and measured volume of the crystal was applied. The indicies of the reflections h, k, l were only cyclicly permutable and included reflections for which $00l = 2n$; these conditions are consistent with Laue class $m\bar{3}$ and with the space groups $I23$, $I2_13$, and $Im\bar{3}$. From analysis the normalized structure factors, it was apparent that the data were centric so they were averaged in $m\bar{3}$ ($R_{ave} = 2.6$) and the refinement was performed in $Im\bar{3}$.

A Patterson map was generated by the use of SHELXS-86 (*6*). The atomic coordinates of each peak in the map were assigned to an atom based on the site multiplicity of the atomic coordinates in space group $Im\bar{3}$

TABLE 1

CRYSTALLOGRAPHIC AND EXPERIMENTAL DATA FOR $[La_{0.86}Cu_3](Ti_{3.42}Al_{0.58})O_{12}$

Space group	$Im\bar{3}$ (No. 204)
a (Å)	7.421 (1)
Volume (Å^3)	408.68 (6)
Z	2
Formula weight	681.6
Calculated density(g/cm^3)	5.54
Temperature (K)	153
Radiation	Graphite-monochromated Mo $K\alpha$ (0.7107 Å)
Linear absorption coefficient (cm^{-1})	147
Secondary extinction coefficient	0.157 E-04
Transmission factors	0.178-0.270
Scan type	$\theta/2\theta$
2θ range (°)	4–89.5
Indices collected	$+h$, $+k$, $+l$
Number of unique data	361
Number of unique data with $I > 3\sigma(I_o)$	253
Number of variables	14
R	0.027
R_w	0.037
Goodness of fit	1.36

and the formula $[La_{4/3}Cu_6](Ti_8)O_{24}$ ($Z = 2$). All atoms were located by the use of the map, and a full-matrix least-squares calculation was used to refine the y and z coordinates for oxygen and the thermal factors for all of the atoms. All calculations were performed by the use of TEXSAN (*7*) crystallographic software. Conventional scattering factors were used (*8*). A corection for anomalous dispersion was applied (*9*).

After the initial refinement, the reliability factors were $R = 0.063$ ($R = [\Sigma(\|F_o| - |F_c\|)/(\Sigma|F_o|)]$) and $R_w = 0.124$ ($R_w = [\Sigma w(|F_o| - |F_c|)^2/(\Sigma w|F_o|^2)]$, $w = 1/\sigma^2(F)$) and the thermal factor for lanthanum was less than 0.1, which suggested that the charge deficit caused by incorporation of aluminum on the titanium site was balanced by excess lanthanum. The lanthanum occupancy was refined and it converged to 0.87. At this point, aluminum was introduced, and, owing to its coordination and geometrical preferences, it was assumed that it was present exclusively on the titanium site. It was not possible to independently refine the occupancies of aluminum and lanthanum because they were strongly coupled to the thermal factors and the scale factor. The lanthanum content and aluminum content were determined from the general formula $[La_{2/3+x/3}\square_{1/3-x/3}Cu_3](Ti_{4-x}Al_x)O_{12}$ by iteration of lanthanum content from 0.87 to 0.84 in 0.01 increments. The minimum reliability factors occurred for a lanthanum content of 0.86 and were $R = 0.027$ and $R_w = 0.037$. The largest peak in the difference map was 2.16 ē/Å^3, and it was not associated with any of the atoms in the structure. Observed and unobserved reflections were included in the final refinement cycle.

Results

Phase Studies

The subsolidus phase diagram of the La_2O_3–CuO–TiO_2 system in air at 960°C contains two ternary compounds La_2CuTiO_6 (*10–13*) and $[La_{2/3}Cu_3](Ti_4)O_{12}$ (*14*);

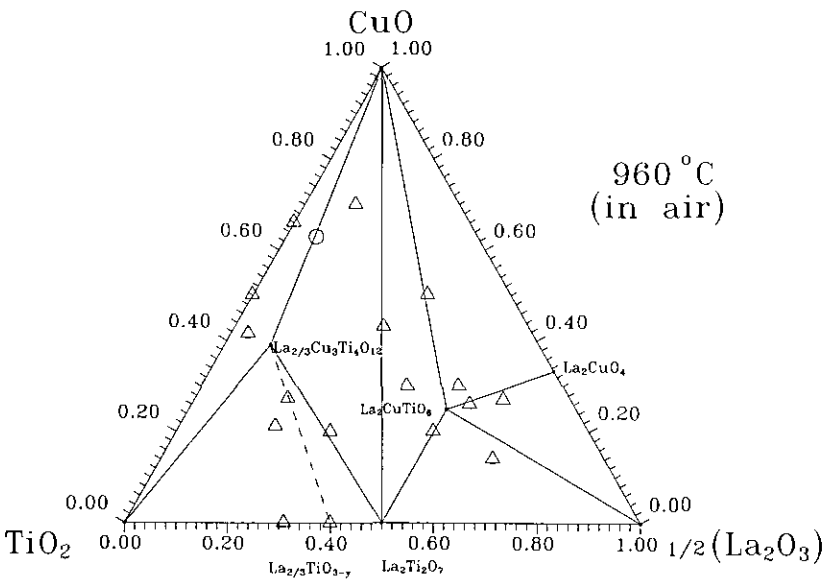

FIG. 1. Subsolidus phase diagram of La_2O_3–CuO–TiO_2 phase diagram in air at 960°C. Triangles represent the compositions used to determine the phase relationships. The circle is the composition of the flux used to grow the single crystals. The triangle on the dotted line contains $La_2Ti_2O_7$ in addition to the phases at either end.

see Fig. 1. The binary systems have been studied previously. The binary systems will be briefly reviewed, and the results from the ternary system will be presented.

CuO–TiO_2 system. Under the experimental conditions, no binary compounds form. The existence of Cu_2TiO_3, Cu_3TiO_4 (*15, 16*) and Cu_3TiO_5 has been postulated (*17, 18*). The existence of Cu_3TiO_4 has been confirmed (*19*), but it is stable only above 867°C and its composition fluctuates between $Cu_3TiO_{4-\delta}$, $-0.3 \leq \delta \leq 0.1$. It was indexed on a hexagonal cell with $a = 3.05$ and $c = 11.5$ Å.

La_2O_3–TiO_2 system. $La_2Ti_2O_7$ and $La_{2/3}TiO_{3-\delta}$ are present. The system (*20*) was originally reported to contain $La_4Ti_9O_{24}$, $La_2Ti_2O_7$, and La_2TiO_5 in air at 1300°C. Later, $La_{2/3}TiO_{3-\delta}$, $0.007 \leq \delta \leq 0.079$, was prepared under a controlled reducing atmosphere ($CO_2/H_2 \leq 2$) at 1350°C (*21*). $La_2Ti_2O_7$ is related to pyrochlore, and is isostructural with $Ca_2Nb_2O_7$. It has been indexed on a monoclinic cell with cell parameters $a = 7.800\,(3)$, $b = 13.011\,(4)$, $c = 5.546\,(2)$ Å, $\gamma = 98.60°\,(2)$, and $Z = 4$ (*22*). $La_{2/3}\square_{1/3}TiO_{3-\delta}$ is an *A*-site and oxygen deficient perovskite. When δ is large it exhibits a cubic perovskite structure; when δ is small it exhibits an orthorhombic structure with the subcell $a = 3.869$, $b = 3.882$, and $c = 3.891$ Å. Under our experimental conditions, it cannot be obtained single phase, as it contains $La_2Ti_2O_7$.

La_2O_3–CuO system. The first member in the homologous series $La_{n+1}Cu_nO_{3n+1-y}$, the familiar La_2CuO_4, forms under the conditions of this study. Structurally, it is very similar to K_2NiF_4. It has been indexed on an orthorhombic cell with cell parameters $a = 5.409$, $b = 5.363$, and $c = 13.17$ Å (*23*).

La_2O_3–CuO–TiO_2 system. This system presents an wide range of reactivities. Owing to the low reactivity of rutile TiO_2, several weeks are required to establish equilibrium in the titanium-rich portion of the diagram. In contrast, equilibrium in the copper-rich region of the phase diagram is

TABLE II

INDEXED X-RAY DIFFRACTION PATTERN OF La_2CuTiO_6[a]

hkl	$d_{calc.}$	$d_{obs.}$	I/I_o	*hkl*	$d_{calc.}$	$d_{obs.}$	I/I_o
110	3.961	3.956	15	213	1.8071	1.8069	1
002	3.921	3.920	10	310/114	1.7570	1.7616	4
111	3.535	3.535	4	131/311	1.7312	1.7332	5
020	2.808	2.808	20	132	1.6170	1.6171	11
112	2.786	2.785	100	024	1.6074	1.6077	21
021	2.644	2.647	2	204	1.6047	1.6032	14
211	2.383	2.380	1	223	1.5785	1.5789	1
103	2.368	2.366	1	133	1.4684	1.4688	2
022	2.283	2.284	8	224	1.3932	1.3923	11
202	2.275	2.270	11	314	1.3128	1.3112	3
113	2.182	2.181	2	331	1.3019	1.3012	1
220	1.980	1.977	17	241	1.2387	1.2398	6
004	1.960	1.961	17	225	1.2295	1.2290	1

[a] Orthorhombic with $a = 5.587$ (6), $b = 5.616$ (5), and $c = 7.842$ (7) Å.

achieved in less than two weeks. The line from $La_{2/3}TiO_{3-\delta}$ to $[La_{2/3}Cu_3](Ti_4)O_{12}$ is dotted because the sample contains a small amount of $La_2Ti_2O_7$ owing to the inability to make the former pure in air. The series of compositions $LaCu_{1-x}Ti_xO_3$ ($0 \leq x \leq 1$), which is of interest in conversion of syngas to oxygenates (*12*), has been studied. It is only single phase at $x = 0.5$.

La_2CuTiO_6

The compound was originally reported (*10*) to belong to a cubic crystal system and have the cell parameter $a = 7.872$ Å, however, we find the compound is orthorhombic and has cell parameters $\sqrt{2}a_o = 7.901$ (6), $\sqrt{2}b_o = 7.942$ (5), and $c_o = 7.842$ (7) Å. We find no evidence of a cubic phase even when synthetic conditions identical to those reported (*10*) are employed. The indexed powder pattern is presented in Table II. The material has orthohombic symmetry and exhibits systematic absences consistent with space group *Pbnm*, namely, $0kl$: $k = 2n + 1$, $h0l$: $h + l = 2n + 1$, $h00$: $h = 2n + 1$, $0k0$: $k = 2n + 1$, and $00l$: $l = 2n + 1$. From comparison of indexed powder patterns, we assume that La_2CuTiO_6 is isostructural with Nd_2CuTiO_6. We determined the structure of the latter (*24*) by Rietveld refinement of time-of-flight powder neutron diffraction collected at the Intense Pulsed Neutron Source at Argonne National Laboratory. Nd_2CuTiO_6 and presumably La_2CuTiO_6 are isostructural with $GdFeO_3$ (*25*). The copper and titanium are disordered over one crystallographic site; see Fig. 2.

La_2CuTiO_6 exhibits Curie-Weiss behavior in the region from 175 to 300 K, an effective moment of 1.2 μ_B, and a Weiss constant of -55 K, see Fig. 3. The data between 175 and 300 K were fit by application of the Curie–Weiss Law, $\chi = \chi_o + C/(T + \theta)$, where χ is the total susceptibility, χ_o is a small, temperature-independent contribution, C is the Curie constant, T is the temperature, and θ is the Weiss constant. The effective moment and Weiss constant differ from that of 1.89 μ_B and -365 K reported previously (*10*). When we employ the same reaction time and synthesis temperature used in the study by Ramadass *et al.* (*10*), we find evidence of La_2CuO_4, which is antiferromagnetic, in the X-ray diffraction pattern. The presence of La_2CuO_4 could ac-

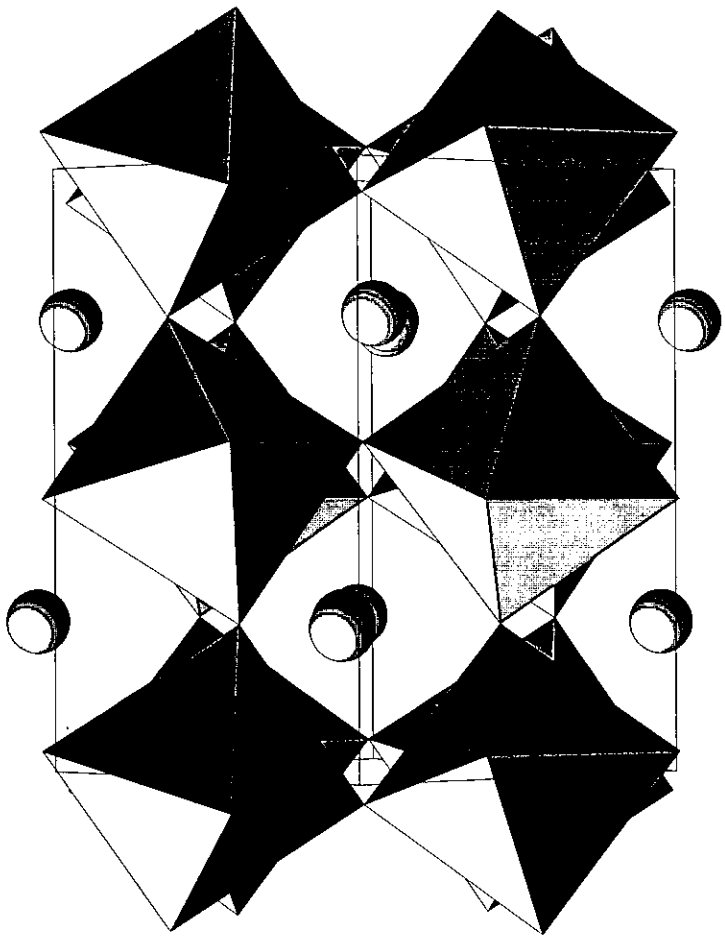

FIG. 2. Idealized polyhedral representation of La_2CuTiO_6 viewed down [110]. The polyhedra are (Cu, Ti)O_6 and the circles are lanthanum.

count for the higher effective moment observed in the previous experiment.

$[La_{0.86}\square_{0.14}Cu_3](Ti_{3.42}Al_{0.58})O_{12}$

The structure is shown in Fig. 4. The compound is a member of a general class of perovskite-related materials $[AC_3](B_4)O_{12}$ (*14, 26*). The compound has lattice parameters that are doubled with respect to cubic perovskite ABO_3. Each lanthanum cation resides inside a 12-coordinate site that is formed by three mutually perpendicular O_4 rectangles of different size; see Fig. 5. Each titanium cation and aluminum cation resides at the center of a $BO_{6/2}$ polyhedron. The BO_6 polyhedra form a tilted corner-shared network similar to that found in $In(OH)_3$ and $Sc(OH)_3$ (*27*). The copper(II) cation is a Jahn–Teller cation and exhibits square planar coordination. Each copper cation occupies what would be an A-cation site in a perovskite. It has eight additional oxygen atoms at greater than 2.5 Å. The eight oxygen atoms form two perpendicular square planes, both of which are perpendicular to

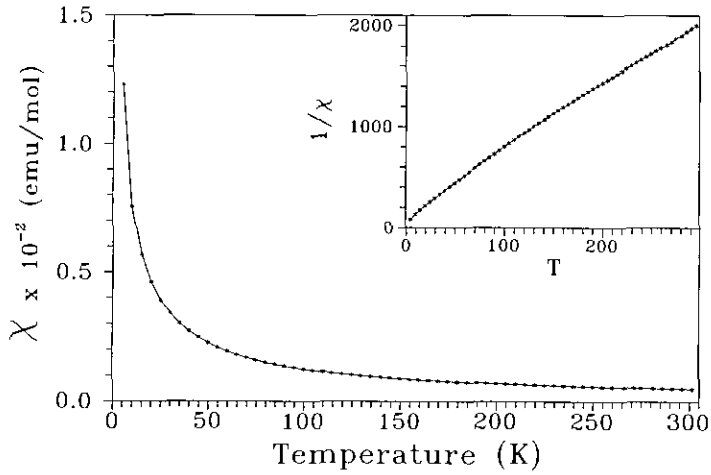

FIG. 3. Molar susceptibility versus temperature for La_2CuTiO_6. The inset shows reciprocal susceptibility versus temperature.

the plane formed by the closest oxygen atoms. The atomic parameters appear in Tables IIIa and IIIb, and selected bond lengths and angles appear in Table IV. Susceptibility measurements exhibit a maximum at about 20 K, which indicates antiferromagnetic order below this temperature; see Fig. 6.

Discussion

The La_2O_3–CuO–TiO_2 system differs from the La_2O_3–CuO–SnO_2 system in three significant ways: (1) The phase relationships in the two systems differ in the lanthanum-rich regions; (2) La_2CuTiO_6 has a random B-cation arrangement; La_2CuSnO_6 has a layered B-cation arrangement; see Fig. 7; (3) The latter does not contain an $[AC_3](B_4)O_{12}$ compound. The last two observations can be attributed to the different size and possibly the different electronic configurations of tin d^{10} and titanium d^0.

In La_2CuSnO_6, the large ionic radius (0.69 Å) (*28*) of tin allows the copper atoms (0.60 Å equatorial) to express a cooperative Jahn–Teller distortion along one crystallographic direction, which leads to a layered structure. In La_2CuTiO_6, the smaller ionic radius of titanium (0.605 Å) requires smaller lattice dimensions. The need for smaller lattice dimensions results in an isotropic compression of the Cu–O bonds and diminishes the Jahn–Teller effect for copper. Without a strong Jahn–Teller distortion around copper

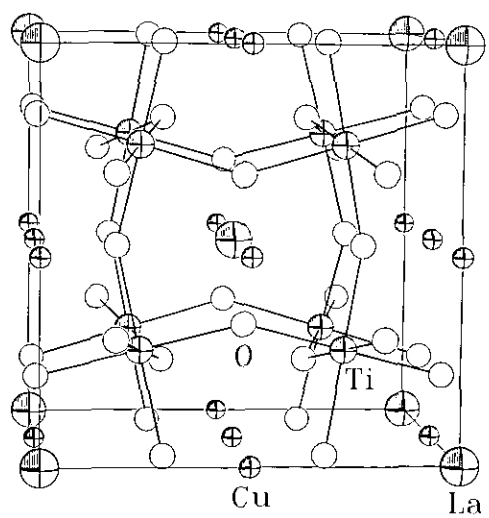

FIG. 4. Structure of $La_{0.86}Cu_3Ti_{3.42}Al_{0.58}O_{12}$ viewed down the c-axis.

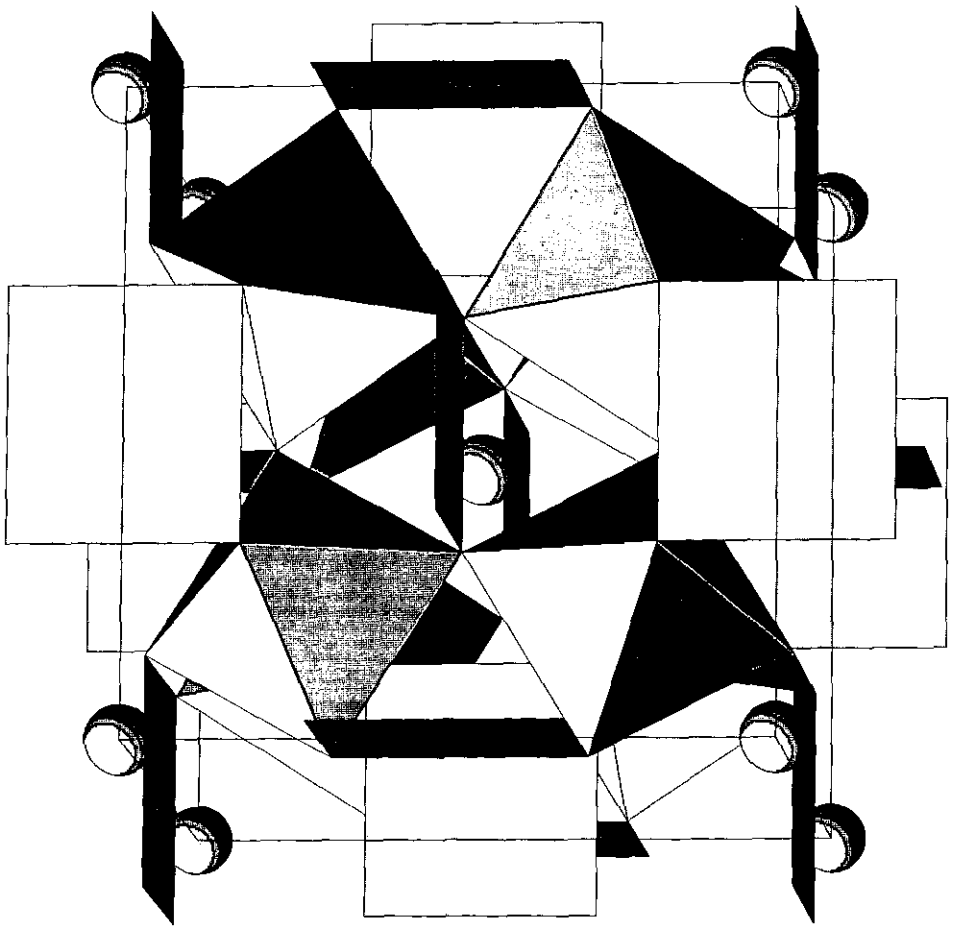

FIG. 5. Idealized depiction of $La_{0.86}Cu_3Ti_{3.42}Al_{0.58}O_{12}$. The titanium atoms are at the centers of the octahedra, the copper atoms are at the centers of the squares, the oxygen atoms are at the vertices of the polyhedra, and the circles are lanthanum atoms.

to provide distinct sites within the lattice, the titanium and copper randomly mix over one crystallographic site.

Tin is evidently too large to form the $[AC_3](B_4)O_{12}$ structure. In $[AC_3](B_4)O_{12}$ compounds the BO_6 octahedra are rotated about an axis perpendicular to $\langle 111\rangle_c$. The *B*–O and nearest C–O bond distances control the tilt angle ϕ (*3*). The greater the *B*–O bond length is relative to the *C*–O bond length, the greater the tilt angle needed to satisfy both bonds. The tilt angle in the La–Cu–Ti–Al–O phase is about 23.5°. The angle is smaller than in other copper titanates, such as $[Tb_{2/3}Cu_3](Ti_4)O_{12}$ (23.8°) (*14*), $[CaCu_3](Ti_4)O_{12}$ (24.1°) (*29*), and $[NdCu_3](Ti_3Fe)O_{12}$ (24.1°) (*30*). The incorporation of tin for titanium would introduce a severe tensile stress on the Cu–O bonds that could be relieved only by a large increase in the tilt angle to about 26°. Apparently the elastic strain from severely tilted octahedra would be too large in this case, and at the composition $\frac{1}{3}$ La_2O_3, 3 CuO, and 4 SnO_2, the combination of $\frac{10}{3}$ SnO_2, 3 CuO, and $\frac{1}{3}$ $La_2Sn_2O_7$ is more favorable than $[La_{2/3}Cu_3](Sn_4)O_{12}$.

The crystal structure of $[La_{0.86}\square_{0.14}$

TABLE IIIa

POSITIONAL AND THERMAL PARAMETERS FOR $[La_{0.86}Cu_3](Ti_{3.42}Al_{0.58})O_{12}$[a]

Atom	Site	$x/\mathbf{a}$ (σx)	$y/\mathbf{b}$ (σy)	$z/\mathbf{c}$ (σz)	B(Å^2)(σB)	Occupancy
La	2*a*	0	0	0	0.185(1)	0.86[b]
Cu	6*b*	0	$\frac{1}{2}$	$\frac{1}{2}$	0.28(2)	1
Ti/Al	8*c*	$\frac{1}{4}$	$\frac{1}{4}$	$\frac{1}{4}$	0.296(1)	0.86/0.14[c]
O	24*g*	0.1805(3)	0.3023(3)	0	0.35(6)	1

[a] Space group $Im\bar{3}$ with a = 7.421 (1) Å and Z = 2.
[b] Refined by TEXSAN then fixed; see text.
[c] Values required for charge balance; see text.

$Cu_3](Ti_{3.42}Al_{0.58})O_{12}$ illustrates the influence that *A*-cation vacancies in conjunction with the choice of crucible have on the final product of a high-temperature crystal growth. In the crystal growth, the growth conditions provided a melt with a significant concentration of aluminum and resulted in the partial substitution of trivalent aluminum for tetravalent titanium. The incorporation of aluminum was not unexpected; several new aluminates, such as $LaSrCuAlO_5$ (*31*) and $Ca_2LaMnAlO_7$ (*32*), have been grown from high-temperature solutions by the use of an alumina crucible as the aluminum source. In the titanate, the incorporated aluminum leads to a charge deficiency of 0.58 per formula unit. Charge neutrality could be provided by three possible mechanisms: (1) loss of oxygen, (2) oxidation of copper(II) to copper(III), (3) occupation of cation vacancies. The general formulas for that result for these three mechanisms are $[La_{2/3}\square_{1/3}Cu_3](Ti_{4-x}Al_x)O_{12-x/2}$, $[La_{2/3}\square_{1/3}Cu^{2+}{}_{3-x}Cu^{3+}{}_x](Ti_{4-x}Al_x)O_{12}$, and $[La_{2/3+x/3}\square_{1/3-x/3}Cu_3](Ti_{4-x}Al_x)O_{12}$.

Mechanism one is unfavorable because it would introduce oxygen defects that would require 5- or 4-coordinate titanium and aluminum, and 3- or 2-coordinate d^9 copper(II) (or introduce crystallographic shear, which is not the case). Mechanism two does not account for the observed incorporation of lanthanum. Mechanism three provides the necessary electrostatic driving force to stabilize the structure. The extra La^{3+} cations, which fill a portion of the *A*-cation vacancies, provide an increased electrostatic interaction and a more favorable lattice

TABLE IIIb

ANISOTROPIC THERMAL PARAMETERS FOR $[La_{0.86}Cu_3](Ti_{3.42}Al_{0.58})O_{12}$

Atom	U_{11}	U_{22}	U_{33}	U_{12}	U_{13}	U_{23}
La	0.0022(2)	0.0022	0.0022	0	0	0
Cu	0.0026(3)	0.0030(3)	0.0051(3)	0	0	0
Ti/Al	0.0037(2)	0.0037	0.0037	0.0012(2)	0.0012	0.0012
O	0.0041(6)	0.0067(8)	0.0026(7)	0.0001(6)	0	0

Note. $U = \exp\{-2\pi^2(a^{*2}U_{11}h^2 + b^{*2}U_{22}k^2 + c^{*}U_{33}l^2 + 2a^{*}b^{*}U_{12}hk + 2a^{*}c^{*}U_{13}hl + 2b^{*}c^{*}U_{23}kl)\}$. $U_{11} = U_{22} = U_{33}$ for La; $U_{12} = U_{13} = U_{23} = 0$ for La and Cu; $U_{11} = U_{22} = U_{33}$; $U_{12} = U_{13} = U_{23}$ for Ti; $U_{13} = U_{23} = 0$ for O.

TABLE IV

DISTANCES[a] AND ANGLES FOR $[La_{0.86}Cu_3](Ti_{3.42}Al_{0.58})O_{12}$[b]

	Bond distances		
La–O	2.613 (2) × 12	Cu–O	1.987 (2) × 4
		–O	2.788 (2) × 4
Ti/Al–O	1.9643 (7) × 6	–O	3.264 (2) × 4
	Bond angles		
O–Cu–O	84.80 (10) × 2	O–Ti/Al–O	89.45 (9) × 6
O–Cu–O	95.20 (10) × 2	O–Ti/Al–O	90.55 (9) × 6

[a] For oxygen atoms within 3.5 Å.

[b] Bond distances in angstroms and bond angles in degrees.

energy. The *B*–O bonding in the corner-shared framework must be compromised owing to local distortions caused by different size (0.53 versus 0.61 Å) and formal charge of the incorporated aluminum. However, the net effect of the incorporation of aluminum and excess lanthanum is the stabilization of the structure.

$[La_{2/3}Cu_3](Ti_4)O_{12}$ has been made as a polycrystalline powder without aluminum by conventional solid-state techniques (*14*). This demonstrates that aluminum and excess lanthanum are not necessary for the formation of this material. The maximum in susceptibility versus temperature occurs at 20 K, which is similar to that of 27 K for $CaCu_3Ti_4O_{12}$ (*33*), and indicates that the *A*-cation vacancies have little affect on the magnetic properties.

The variable lanthanum content in the single crystals, which compensates the excess framework charge owing to aluminum substitution for titanium, underscores the diversity of defect chemistry in $[AC_3](B_4)O_{12}$ compounds. The presence of the A cation is not necessary for the formation of stable materials. Materials with copper as a *C* cation and titanium plus other small cations as

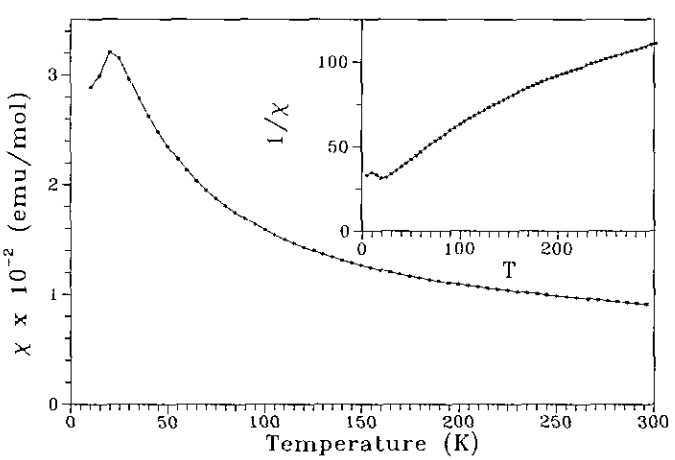

FIG. 6. Molar susceptibility versus temperature for $La_{0.86}Cu_3Ti_{3.42}Al_{0.58}O_{12}$. The inset shows reciprocal susceptibility versus temperature.

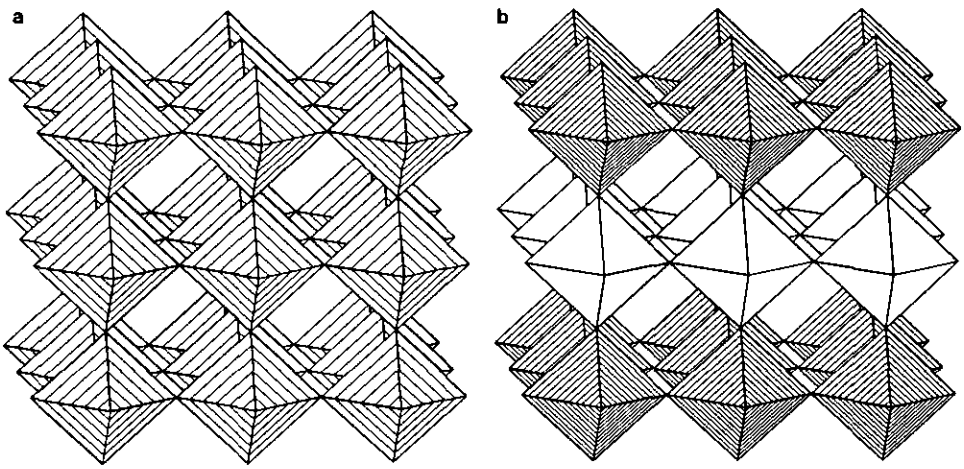

FIG. 7. Idealized polyhedral representation of (a) the disordered arrangement of *B* cations found in La_2CuTiO_6 (b) the layered arrangement of *B* cations found in La_2CuSnO_6.

B cations form with the *A* site unoccupied, as in $[\square Cu_3](M_2Ti_2)O_{12}$ (M = Ta, Nb, Sb) (*14*), partially occupied, as in $[Ln_{2/3}\square_{1/3}Cu_3](Ti_4)O_{12}$ (*14*), and completely occupied, as in $[CaCu_3](Ti_4)O_{12}$ (*29*). It appears that the role of the A cation is primarily to provide charge balance and additional electrostatic stability.

Conclusions

The smaller size of titanium compared with tin is sufficient to change the phase relationships and number of ternary phases in the La_2O_3–CuO–TiO_2 system relative to the La_2O_3–CuO–SnO_2 system as well as the crystal chemistry of La_2CuTiO_6 relative to La_2CuSnO_6. The defect chemistry of $[A_{1-x}C_3](B_4)O_{12}$ ($0 \leq x \leq 1$) compounds and the use of an alumina crucible allows the growth of single crystals that contain aluminum on the *B* (titanium) site and excess lanthanum on the *A* site. The incorporated aluminum does not affect the crystal symmetry compared to the parent $[La_{2/3}Cu_3](Ti_4)O_{12}$, but certainly causes small local distortions of the framework.

Acknowledgments

This work was funded by the National Science Foundation and the Science and Technology Center for Superconductivity, in particular, the Summer Undergraduate Research Program (*VEB*) (*NSF-DMR-8809854*). We gratefully acknowledge C. L. Stern and J. T. Vaughey for their assistance with the single-crystal structure and for helpful discussions. We also acknowledge the Northwestern Materials Research Center for support of the X-ray Diffraction Facility (MRL-DMR-8821571).

References

1. M. T. ANDERSON AND K. R. POEPPELMEIER, *Chem. Mater.* **3,** 476 (1990).
2. A. F. WELLS, "Structural Inorganic Chemistry, Fourth Edition," Oxford, New York (1975).
3. B. G. HYDE AND S. ANDERSSON, "Inorganic Crystal Structures," Wiley, New York (1989).
4. A. I. SHEINKMAN, V. T. MUKHIN, L. M. GOL'DSHTEIN, AND G. V. KLESHSCHEV, *Neorg. Mat.* **6(9),** 1660 (1970).
5. J. DE MEULENAER AND H. TOMPA, *Acta. Crystallogr.* **19,** 1014 (1965).
6. G. M. SHELDRICK, *in* "Crystallographic Computing 3" (G. M. Sheldrick, C. Kruger, and R. Goddard, Eds.), *p. 175*, Oxford (1985).
7. TEXSAN: "Single Crystal Structure Analysis Software Version 5.0," Molecular Structure Corp., The Woodlands, TX (1989).
8. D. T. CROMER AND J. T. WABER, *in* "International

Tables for X-ray Crystallography," Vol. 4, p. 99, Kynoch Press, Birmingham, England (1974).
9. J. A. IBERS AND W. C. HAMILTON, *Acta Crystallogr.* **17,** 781 (1964).
10. N. RAMADASS, J. GOPALAKRISHNAN, AND M. V. C. SASTRI, *J. Inorg. Nucl. Chem.* **40,** 1453 (1978).
11. O. M. PARKASH, D. KUMAR, D. K. GANGOPADHAYAY, AND D. BAHADUR, *Phys. Status Solidi* **96,** K79 (1986).
12. M. L. ROJAS AND J. L. G. FIERRO, *J. Solid State Chem.* **89,** 299 (1990).
13. V. R. SASTRI, R. PITCHAI, AND C. S. SWAMY, *Indian J. Chem.* **19A,** 738 (1980).
14. B. BOCHU, M. N. DESCHIZEAUX, J. C. JOUBERT, J. COLLOMB, J. CHENAVAS, AND M. MAREZIO, *J. Solid State Chem.* **29,** 291 (1979).
15. N. G. SCHMAHL AND F. MÜLLER, *Z. Anorg. Allg. Chem.* **332,** 12 (1964).
16. F. MÜLLER, Thesis, RWTH, Aachen (1960).
17. A. A. SLOBODOYANYUK, YU. D. TRET'YAKOV, AND A. F. BESSONOV, *Russ. J. Inorg. Chem.* **17,** 922 (1972).
18. AMIN, RAJNIKANT BABUBHAI, German patent 2 33 318 (1974).
19. D. HENNINGS, *J. Solid State Chem.* **31,** 275 (1980).
20. J. B. MACCHESNEY AND H. A. SAUER, *J. Am. Ceram. Soc.* **45**(9), 416 (1962).
21. M. ABE AND K. UCHINO, *Mater. Res. Bull.* **9,** 147 (1974).
22. M. GASPARIN, *Acta Crystallogr., Sect B* **31,** 2129 (1975).
23. D. M. DE LEEUW, C. A. H. A. MUTSAERS, G. P. J. GEELEN, AND C. LANGEREIS, *J. Solid State Chem.* **80,** 276 (1989).
24. M. T. ANDERSON AND K. R. POEPPELMEIER, manuscript in preparation.
25. S. GELLER, *J. Chem. Phys.* **24,** 1236 (1956).
26. M. MAREZIO, P. D. DERNIER, J. CHENAVAS, AND J. C. JOUBERT, *J. Solid State Chem.* **6,** 16 (1973).
27. K. SCHUBERT AND A. SEITZ, *Z. Anorg. Allg. Chem.* **256,** 226 (1948).
28. R. D. SHANNON, *Acta Crystallogr., Sect A* **32,** 751 (1976).
29. A. DESCHANVRES, B. RAVEAU, AND T. TOLLEMER, *Bull. Soc. Chim. Fr.,* 4077 (1967).
30. C. MEYER, Y. GROS, B. BOCHU, A. COLLOMB, J. CHENAVAS, J. C. JOUBERT, AND M. MAREZIO, *Phys. Status Solidi* **48,** 581 (1978).
31. J. B. WILEY, M. SABAT, S.-J. HWU, K. R. POEPPELMEIER, A. RELLER, AND T. WILLIAMS, *J. Solid State Chem.* **87,** 250 (1990).
32. M. T. ANDERSON, J. T. VAUGHEY, AND K. R. POEPPELMEIER, manuscript in preparation.
33. A. COLLOMB, D. SAMARAS, B. BOCHU, AND J. C. JOUBERT, *Phys. Status Solidi* **41,** 459 (1977).